*Progress In Electromagnetics Research C, Vol. 123, 253–262, 2022*

# A Ku-Band Low-Profile Dual Circularly Polarized Antenna Based on QMSIW

**Jingchun Zhai[1], Wen Wang[1], Cheng Chang[1], Yiqing Liu[2], Luzhen Wang[3], and Zhuopeng Wang[1, *]**

**Abstract**—In this paper, a low-profile dual circularly polarized (CP) antenna for Ku band satellite communication is proposed. A quarter-mode SIW (QMSIW) is designed as a circular polarization unit, which realizes circular polarization by using high-order mode $TE_{130}$, and a pair of units are combined to form the antenna proposed in this paper. Feeding different units can realize left-handed circular polarization and right-handed circular polarization, respectively. The antenna impedance bandwidth is 5.66 GHz (15.16 GHz–20.82 GHz); the circular polarization bandwidth (CPBW) is 540 MHz (15.64 GHz–16.18 GHz); and the gain in the passband is 5.1 dBi, with a minimum axial ratio (AR) of 1 dB. The thickness of the antenna is only 1.5 mm, which has obvious low-profile characteristics.

## 1. INTRODUCTION

Satellite communications make extensive use of the Ku-band of the electromagnetic spectrum. Antennas are an important part of satellite communication systems, and low-profile antennas are invaluable for some Ku-band satellite applications where antenna space is limited [1, 2]. Substrate integrated waveguides (SIW) enable the creation of high-performance (active and passive) microwave components in planar form, which has become a new field for the design of low-profile antennas. For the consideration of low profile or miniaturization, half-mode SIW (HMSIW), quarter-mode SIW (QMSIW) and eighth-mode SIW (EMSIW) are successively applied to antenna design. In [3], a V-band leaky-wave antenna operating at 55–65 GHz was constructed using HMSIW with a gain up to 14.5 dBi. A compact microstrip Yagi antenna based on HMSIW was proposed in [4], achieving a relative bandwidth of 10.8% while achieving miniaturization. Introducing slits on a QMSIW structure can achieve the purpose of multi-frequency [5, 6] and increase the bandwidth [7]. A bandwidth of 414 MHz was measured in [8] using two eight-mode resonators coupled to each other and exhibiting elliptical polarization. In [9], an HMSIW circularly polarized antenna was fabricated by etching half-octagonal grooves, and the QMSIW circularly polarized antenna was fabricated by dividing the HMSIW in half. [10] proposed a compact planar CP antenna based on a QMSIW subarray, which achieved an AR bandwidth of 5.8%. But it needs to provide a phase difference through a complex feed network to generate circular polarization. [11] proposed a high front-to-back ratio circularly polarized planar antenna based on a QMSIW subarray with a very complex feed network. At the center frequency of 5.2 GHz, the measured 10 dB return loss and 3 dB axial ratio bandwidth are 21.53% and 10.96%, respectively. [12] introduced SIW, HMSIW, and QMSIW in detail, and found that QMSIW can generate circularly polarized waves in $TE_{220}$ mode. This provides a new way for the generation of circular polarization in QMSIW. [13] proposed a broadband dual

*Received 22 July 2022, Accepted 22 August 2022, Scheduled 8 September 2022*

* Corresponding author: Zhuopeng Wang (wzhuopeng1@sdust.edu.cn).

[1] College of Electronic and Information Engineering, Shandong University of Science and Technology, China. [2] College of Electrical Engineering and Automation, Shandong University of Science and Technology, China. [3] China Unicom (Tsingtao), China Unicom, China.

circularly polarized SIW antenna, where the circular polarization is obtained by the $TE_{220}$ mode of a quarter-mode resonator.

This paper proposes a circular polarization QMSIW structure using $TE_{130}$ mode and combines two circularly polarized elements to form a low-profile dual circularly polarized QMSIW antenna. The rest of this paper is organized as follows. Section 2 introduces the structure and evolution process of the antenna in detail and analyzes the principle of the circular polarization generated by the QMSIW structure. The parameters of the QMSIW unit and proposed antenna are studied in Section 3. The antenna prototype was fabricated and measured, and the results are displayed in Section 4. Finally, a conclusion is made in Section 5.

## 2. ANTENNA STRUCTURE AND DESIGN

### 2.1. Antenna Structure

The antenna structure proposed in this paper is shown in Figure 1. The antenna width is $W$, which is obtained by combining two mirror-symmetric proposed QMSIWs. Use Rogers RO4003 (permittivity $\varepsilon_r = 3.55$ and loss tangent $\tan\delta = 0.0027$) as the dielectric substrate with a thickness of $h$. Coaxial feeds are used at the same position of the two QMSIWs. Left-handed circular polarization (LHCP) or right-handed circular polarization (RHCP) can be achieved by choosing different feeding points which are respectively on a symmetry axis of the antenna. The distance between the feeding point and the nearest side of SIW is $l$. The via diameter is $d$, and the spacing between adjacent vias is $p$. There are square notches with widths $w_1$ at the two corners and $w_2$ at the center of the antenna, respectively. The dimensions of the proposed antenna are shown in Table 1.

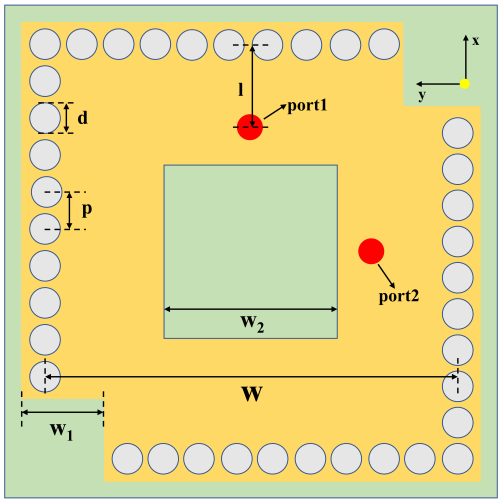


**Figure 1.** The geometry of the proposed CP antenna.

**Table 1.** The specific dimensions of the proposed antenna.

| Parameter | $W$ | $W_1$ | $W_2$ | $l$ |
|---|---|---|---|---|
| Dimension (mm) | 13.2 | 3.45 | 6.5 | 2.2 |
| Parameter | $d$ | $p$ | $h$ | |
| Dimension (mm) | 0.9 | 1.1 | 1.5 | |

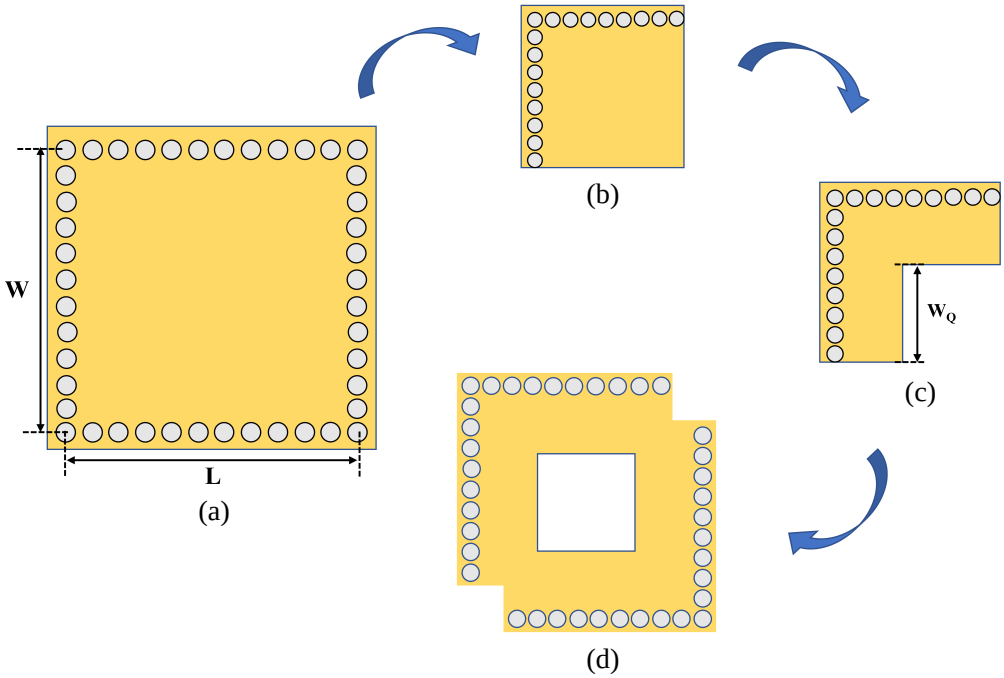


**Figure 2.** Antenna design flow. (a) Rectangular SIW, (b) QMSIW, (c) proposed QMSIW circularly polarized unit, (d) the proposed antenna.

### 2.2. Design Process

Figure 2 shows the evolution of the antenna. First, a rectangular SIW with a length of 19.8 mm and a width of 18.8 mm is designed. The resonant frequency of each mode of the SIW can be obtained by the following formulae [14]:

$$f_{mnq}^{\mathrm{SIW}} = \frac{1}{2\pi\sqrt{\mu\epsilon}}\sqrt{\left(\frac{m\pi}{L_{eff}^{\mathrm{SIW}}}\right)^2 + \left(\frac{n\pi}{W_{eff}^{\mathrm{SIW}}}\right)^2 + \left(\frac{q\pi}{h}\right)^2} \tag{1}$$

$$\begin{cases} L_{eff}^{\mathrm{SIW}} = L - 1.08\dfrac{d^2}{p} + 0.1\dfrac{d^2}{L} \\ W_{eff}^{\mathrm{SIW}} = W - 1.08\dfrac{d^2}{p} + 0.1\dfrac{d^2}{W} \end{cases} \tag{2}$$

where $m = 1, 2, \ldots$, $n = 1, 2, \ldots$, $q = 1, 2, \ldots$, $\mu = \mu_0\mu_r$ is the permeability of the dielectric substrate; $\epsilon = \epsilon_0\epsilon_r$ is the dielectric constant of the substrate; and $H$ is the thickness of SIW. $L_{eff}^{\mathrm{SIW}}$ and $W_{eff}^{\mathrm{SIW}}$ are the effective length and width of SIW, respectively. The difference between the height and width of SIW is too large, and the default $q$ is 0. $L$ and $W$ are the length and width of the SIW; $d$ is the diameter of the metal via; and $p$ is the spacing between adjacent vias. In order to prevent energy leakage, the size and spacing of vias are clearly specified as follows [15]:

$$\begin{cases} \dfrac{p}{d} < 2 \\ \dfrac{d}{W} < 0.2 \end{cases} \tag{3}$$

It can be calculated that the $\mathrm{TE}_{110}$ of the SIW is at 6.1 GHz. Other high-order modes are calculated and listed in Table 2. Figure 3 shows the input impedance simulation results and the field distribution of SIW in each mode.

**Table 2.** Resonant frequency (GHz) of SIW modes.

| m \ n | 1 | 2 | 3 |
|---|---|---|---|
| 1 | 6.1 | 9.52 | 13.25 |
| 2 | 9.5 | 12.05 | 14.8 |

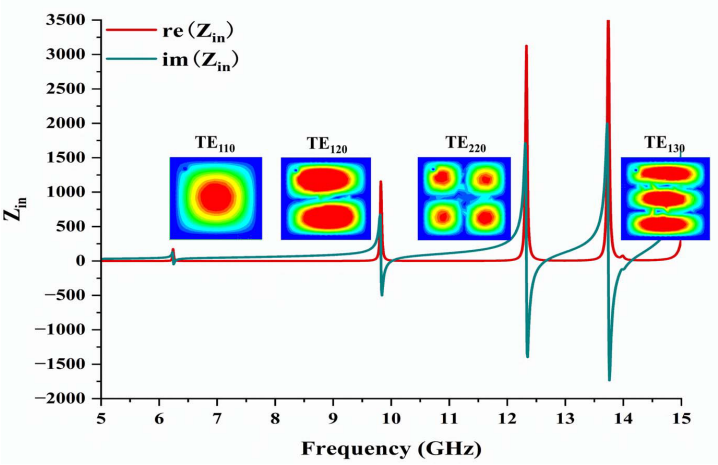


**Figure 3.** SIW input impedance and electric field distribution in each mode.

Cutting along the virtual magnetic wall, QMSIW is generated, as shown in Figure 2(b). According to the calculation method of HMSIW, the effective width of QMSIW can be obtained as [16]

$$W_{eff}^{\mathrm{QMSIW}} = \frac{W_{eff}^{\mathrm{SIW}}}{2} + \Delta W \tag{4}$$

$$\Delta W = h * \left(0.05 + \frac{0.3}{\epsilon_r}\right) * \ln\left(0.79\,\frac{W_{eff}^{\mathrm{SIW}}}{4h^3} + \frac{52W_{eff}^{\mathrm{SIW}} - 261}{h^2} + \frac{38}{h} + 2.77\right) \tag{5}$$

where $W_{eff}^{\mathrm{QMSIW}}$ is the effective width of SIW, and $\Delta W$ is a correction amount. According to formulas (1) and (4), the resonance frequency of each mode of QMSIW can be obtained as

$$f_{mnq}^{\mathrm{QMSIW}} = \frac{1}{2\pi\sqrt{\mu\epsilon}}\sqrt{\left(\frac{m\pi}{2L_{eff}^{\mathrm{QMSIW}}}\right)^2 + \left(\frac{n\pi}{2W_{eff}^{\mathrm{QMSIW}}}\right)^2 + \left(\frac{p\pi}{h}\right)^2} \tag{6}$$

where $m = 1, 2, \ldots$, $n = 1, 2, \ldots$, $q$ is 0 due to the large difference between height and width. The QMSIW used in this paper is different from the regular triangular QMSIW, and this paper deals with higher-order modes of the QMSIW, so it is necessary to explore what modes the rectangular QMSIW can contain. Figure 4 shows the input impedance and electric field distribution of the QMSIW.

It can be seen from Figure 4 that the QMSIW does not have $\mathrm{TE}_{120}$ and $\mathrm{TE}_{220}$ modes, but directly converts from the $\mathrm{TE}_{110}$ to $\mathrm{TE}_{130}$ mode after increasing the frequency. Two open edges of the rectangular QMSIW can be used as virtual magnetic walls for modes $\mathrm{TE}_{110}$ and $\mathrm{TE}_{130}$, and the field distributions of $\mathrm{TE}_{110}$ and $\mathrm{TE}_{130}$ do not change.

A rectangle with a width of $W_Q$ is removed from the corner of the open edge of the QMSIW to form the circularly polarized unit designed in this paper, as shown in Figure 2(c). When $W_Q = 4\,\mathrm{mm}$, the $S_{11}$ of the circularly polarized unit is shown in Figure 5(a), and the unit forms broadband of 3.22 GHz (10.07 GHz–13.29 GHz) by two resonances. From the electric field distribution in Figure 5(c), it can be determined that these two resonances are generated by $\mathrm{TE}_{110}$ and $\mathrm{TE}_{130}$, respectively. The $\mathrm{TE}_{110}$ and

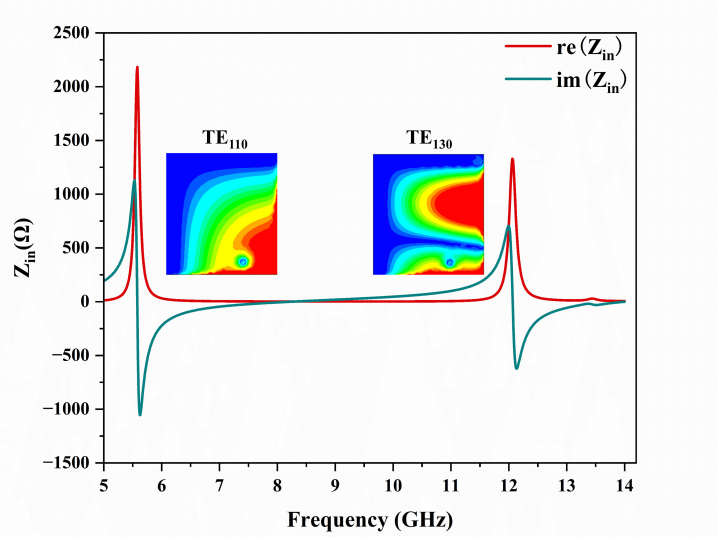


**Figure 4.** The input impedance and electric field distribution of the QMSIW.

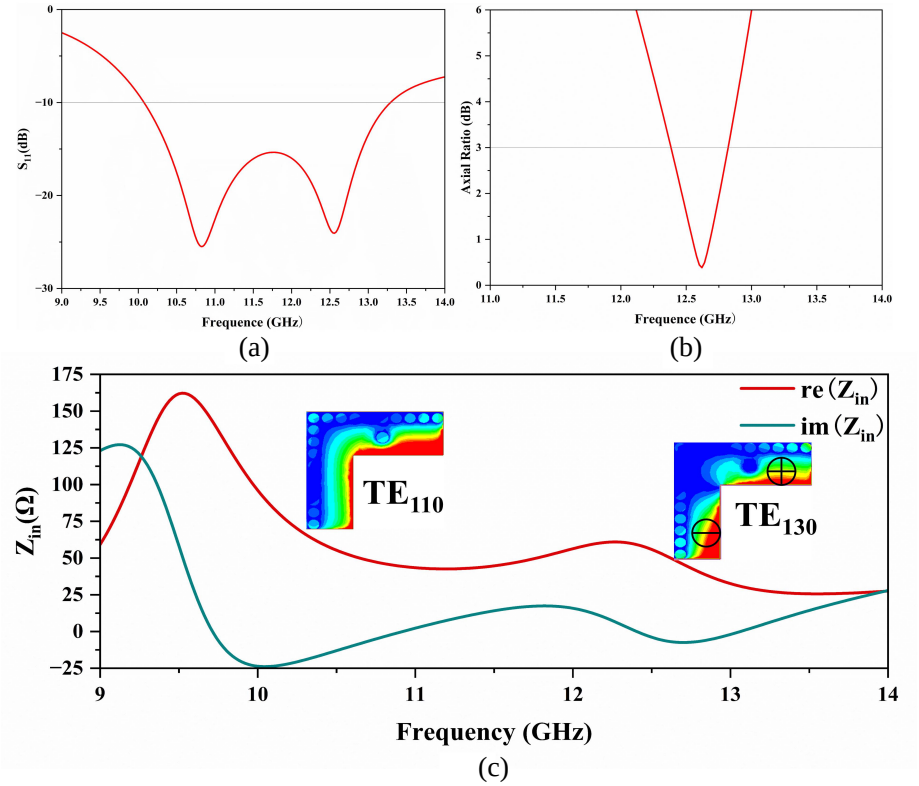


**Figure 5.** QMSIW circular polarization unit (a) $S_{11}$, (b) axial ratio, (c) input impedance and electric field distribution.

$TE_{130}$ modes can still be maintained by removing the rectangle, but removing the rectangle makes the $TE_{130}$ field distribution of QMSIW not the same as that of SIW exactly. The two electric fields of the $TE_{130}$ have the same strength and a phase difference of 90° within a certain frequency, so the QMSIW unit can achieve circular polarization. The axis ratio of this unit is shown in Figure 5(b), and it can be seen that the axial ratio is less than 3 dB at 12.4 GHz–12.8 GHz.

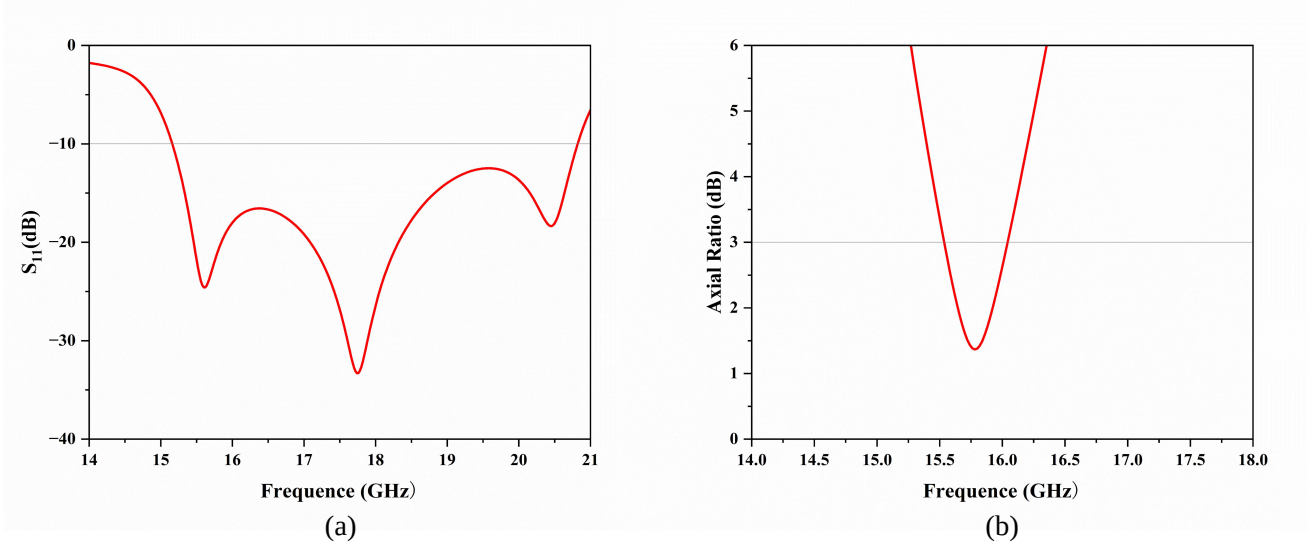


**Figure 6.** Proposed antenna (a) $S_{11}$, (b) axial ratio.

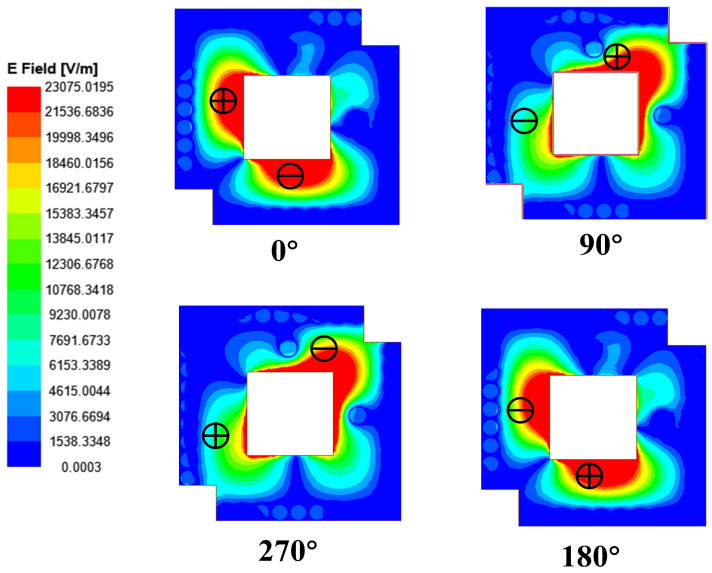


**Figure 7.** Electric field distribution of proposed antenna for $\omega t = 0°$, 90°, 180° and 270° at 15.8 GHz.

The proposed SIW antenna can be obtained by combining a pair of proposed circularly polarized units mirror-symmetrically, and the physical dimensions are given in Table 1. As with the proposed QMSIW unit, the proposed antenna concentrates electric fields with the same amplitude and 90° phase difference on the two open edges, thereby achieving circular polarization. The $S_{11}$ and axial ratios of the antennas are given in Figures 6(a) and (b), respectively. Due to the mutual coupling of the two QMSIW circularly polarized units, the resonance and axial ratio minimum frequencies are moved to higher frequencies. The electric field distribution of the proposed antenna for $\omega t = 0°$, 90°, 180°, and 270° at 15.8 GHz is shown in Figure 7. It can be seen that the two electric fields with different phases rotate around the open edge.

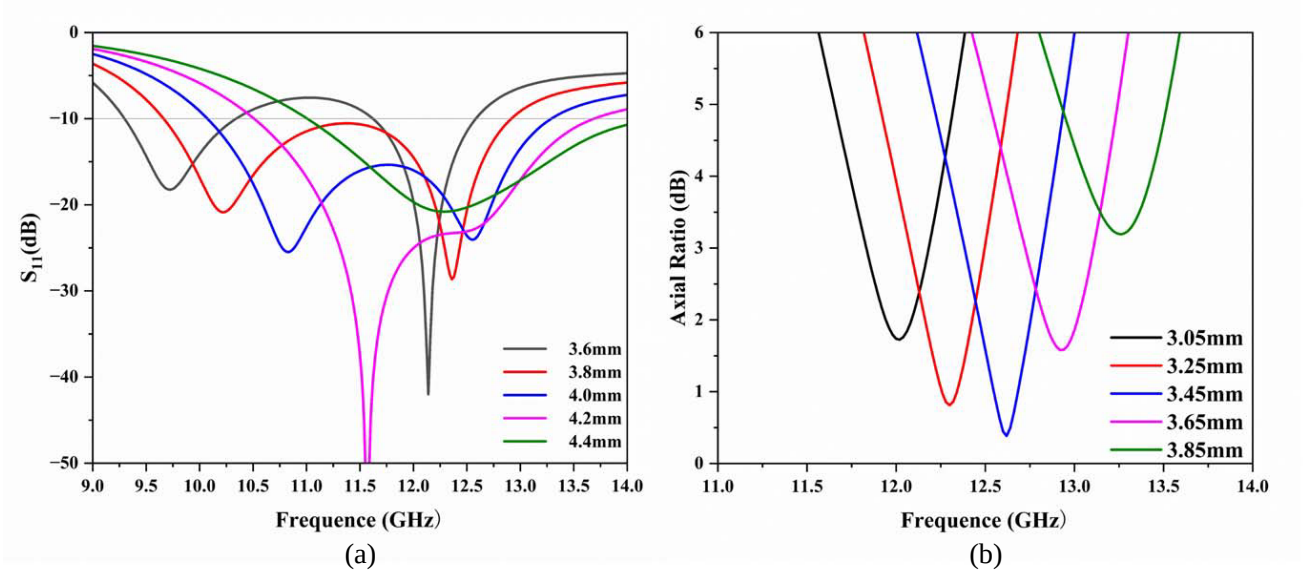


**Figure 8.** Comparison of (a) $S_{11}$ and (b) axial ratios with different sizes of $W_Q$.

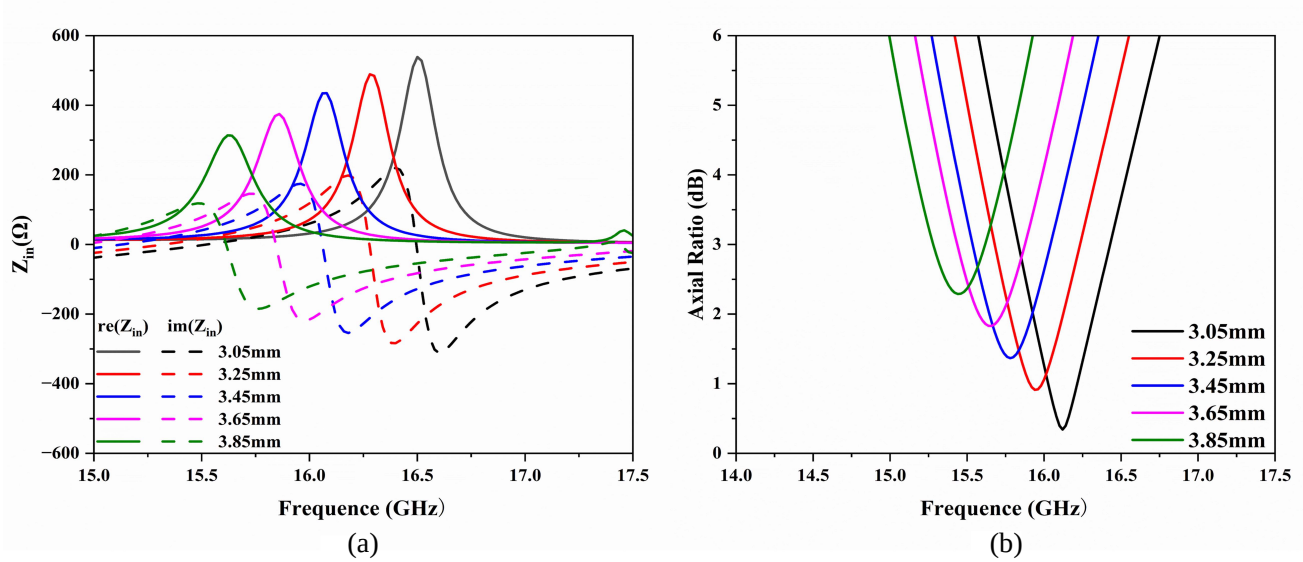


**Figure 9.** Comparison of (a) input impedance and (b) axial ratios with different sizes of $W_1$.

## 3. PARAMETRIC STUDIES

$W_Q$ of the proposed QMSIW circularly polarized unit and $W_1$ of the proposed antenna are selected for parametric studies.

Figure 8(a) shows the change of $S_{11}$ when $W_Q$ is changed. In the process of increasing the $W_Q$ from 3.6 mm to 4.4 mm, it can be found that the resonant frequency of $TE_{110}$ is getting higher and higher, while the resonant frequency of $TE_{130}$ moves a little. When the resonant frequency of $TE_{110}$ is close to that of $TE_{130}$, a wide band is formed. Figure 8(b) shows the variation of the axial ratio with $W_Q$. It can be seen that the minimum frequency of the axial ratio increases with the increase of $W_Q$ and is always consistent with the $S_{11}$ resonance of the $TE_{130}$.

The change of $W_1$ can be understood as the change of the coincidence degree of the two QMSIW units, which directly determines the coupling of the two units. Figure 9(a) shows the variation of

input impedance with $W_1$. It can be seen that the resonant frequency moves to a low frequency as $W_1$ increases. Figure 9(b) shows the change in the axial ratio with $W_1$. Restricted by factors such as SMA connector size and fabricating, two units cannot overlap infinitely, so 3.45 mm is chosen as the actual fabricating size as a compromise.

## 4. SIMULATION AND MEASURED RESULTS

The proposed antenna was fabricated and measured for verification of the design. The simulated and measured results of $S_{11}$, AR, and gain are shown in Figure 10. The measurements show an impedance

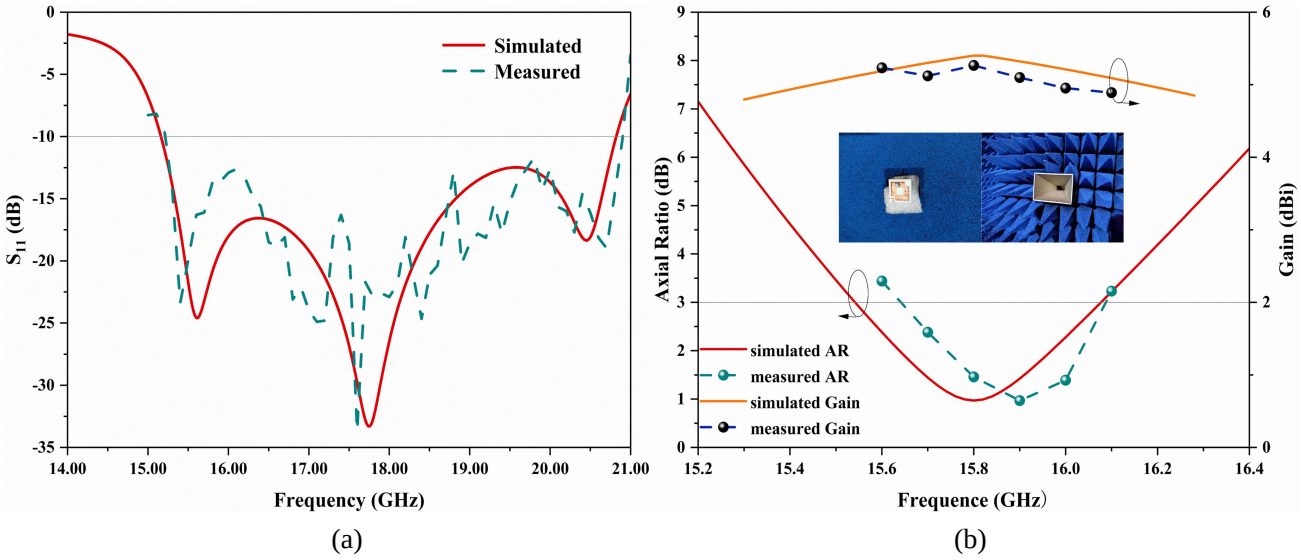


**Figure 10.** Simulated and measured (a) $S_{11}$, (b) axial ratio and gain.

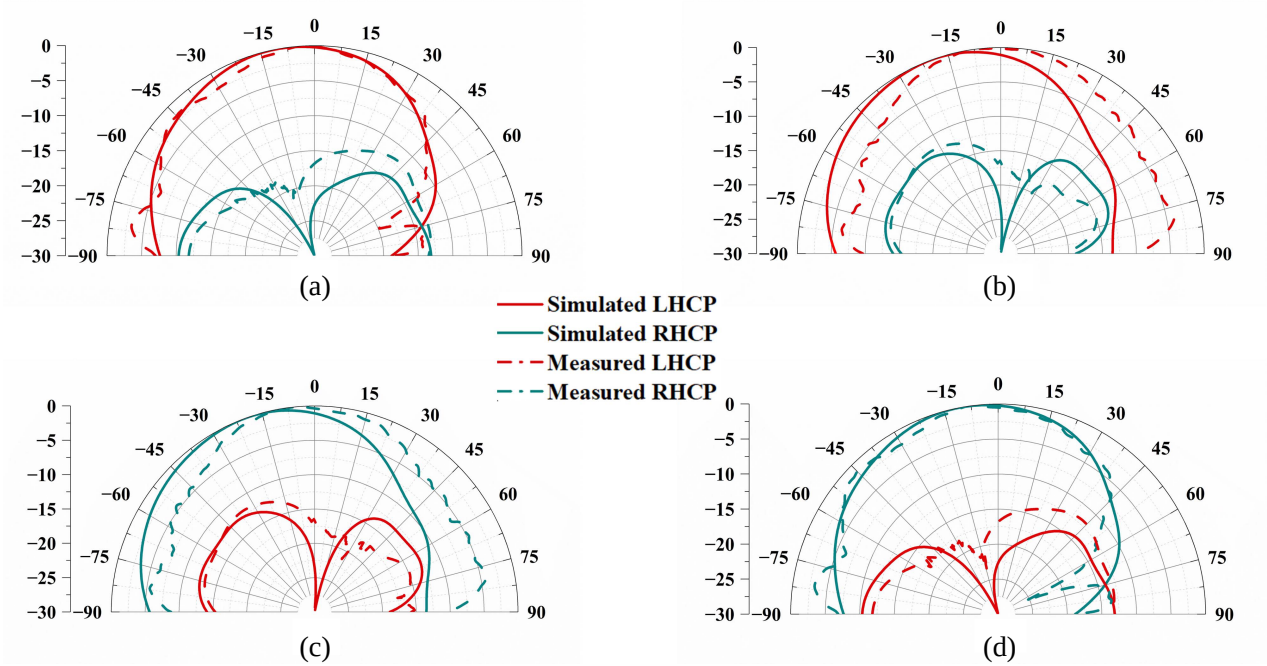


**Figure 11.** (a) $E$-plane fed by port 1 at 15.8 GHz, (b) $H$-plane fed by port 1 at 15.8 GHz, (c) $E$-plane fed by port 2 at 15.8 GHz, (d) $H$-plane fed by port 2 at 15.8 GHz.

bandwidth (IBW) of 31.46% [5.66 GHz (15.16 GHz–20.82 GHz)], CPBW of 3.39% [540 MHz (15.64 GHz–16.18 GHz), and a peak gain of 5.1 dBi fed by port 1. Figure 11 shows the simulated and measured radiation patterns of the proposed antenna using different feed points at 15.8 GHz. Due to errors in antenna fabrication and measurement, there are some differences between simulated and measured results, which is still acceptable.

## 5. CONCLUSION

A low-profile dual circularly polarized antenna for Ku-band satellite communication is proposed. A QMSIW unit using $TE_{130}$ mode to realize circular polarization is designed, and the principle of circular polarization is analyzed. Combining two identical units constitutes the SIW antenna proposed in this paper. Left-handed circular polarization and right-handed circular polarization can be achieved respectively by feeding different units. The antenna is fabricated and measured. The IBW of the antenna is 5.66 GHz (15.16 GHz–20.82 GHz); the CPBW is 540 MHz (15.64 GHz–16.18 GHz); and the in-band gain is 5.1 dBi. The thickness of the antenna is only 1.5 mm, which has obvious low-profile characteristics. The results show that the proposed antenna is an excellent candidate for Ku-band satellite applications.

## REFERENCES

1. Asci, Y., M. Pehlivan, and K. Yegin, "Dual cavity Ku-band antenna for SatCom applications," *2017 25th Telecommunication Forum (TELFOR)*, 1–3, 2017, doi: 10.1109/TELFOR.2017.8249380.
2. Zhai, J., G. Chen, W. Wang, Y. Liu, L. Wang, and Z. Wang, "A novel low profile circularly polarized GNSS antenna with wide 3 dB axial ratio beamwidth," *Progress In Electromagnetics Research M*, Vol. 111, 199–208, 2022.
3. Sarkar, A. and S. Lim, "60 GHz compact larger beam scanning range PCB leaky-wave antenna using HMSIW for millimeter-wave applications," *IEEE Transactions on Antennas and Propagation*, Vol. 68, No. 8, 5816–5826, Aug. 2020, doi: 10.1109/TAP.2020.2983784.
4. Zhang, Z., G. Zhang, X. Cao, J. Gao, H. Yang, and J. Wu, "Compact microstrip Yagi antenna based on half-mode substrate integrated waveguide," *2016 IEEE International Conference on Microwave and Millimeter Wave Technology (ICMMT)*, 737–739, 2016, doi: 10.1109/ICMMT.2016.7762426.
5. Alvarez, M., C. Kalialakis, F. Mira, and S. K. Goudos, "A dual band antenna based on a quarter mode substrate integrated waveguide," *2017 6th International Conference on Modern Circuits and Systems Technologies (MOCAST)*, 1–4, 2017, doi: 10.1109/MOCAST.2017.7937621.
6. Ali, M., K. K. Sharma, and R. P. Yadav, "Design of compact dual band quarter mode SIW cavity backed slot antenna," *2017 International Conference on Inventive Computing and Informatics (ICICI)*, 888–890, 2017, doi: 10.1109/ICICI.2017.8365264.
7. Chaturvedi, D. and S. Raghavan, "A quarter-mode SIW based antenna for ISM band application," *2017 IEEE International Conference on Antenna Innovations & Modern Technologies for Ground, Aircraft and Satellite Applications (iAIM)*, 1–4, 2017, doi: 10.1109/IAIM.2017.8402617.
8. Agneessens, S., "Coupled eighth-mode substrate integrated waveguide antenna: Small and wideband with high-body antenna isolation," *IEEE Access*, Vol. 6, 1595–1602, 2018, doi: 10.1109/ACCESS.2017.2779563.
9. Tian, S., H. Tang, X. Guan, W. Xu, Y. Wu, and K. Kang, "A novel circularly polarized half-mode/quarter-mode SIW antenna," *2021 IEEE 4th International Conference on Electronics Technology (ICET)*, 668–671, 2021, doi: 10.1109/ICET51757.2021.9450943.
10. Jin, C., Z. Shen, R. Li, and A. Alphones, "Compact circularly polarized antenna based on quarter-mode substrate integrated waveguide sub-array," *IEEE Transactions on Antennas and Propagation*, Vol. 62, No. 2, 963–967, Feb. 2014, doi: 10.1109/TAP.2013.2291574.
11. Ran, Y., Y. Peng, and J. Li, "A circularly polarized antenna based on EMSIW sub-array with high front-to-back ratio," *2015 16th International Conference on Electronic Packaging Technology (ICEPT)*, 1390–1393, 2015, doi: 10.1109/ICEPT.2015.7236839.

12. Jin, C., R. Li, A. Alphones, and X. Bao, "Quarter-mode substrate integrated waveguide and its application to antennas design," *IEEE Transactions on Antennas and Propagation*, Vol. 61, No. 6, 2921–2928, Jun. 2013, doi: 10.1109/TAP.2013.2250238.
13. Kumar, K., S. Dwari, and M. K. Mandal, "Broadband dual circularly polarized substrate integrated waveguide antenna," *IEEE Antennas and Wireless Propagation Letters*, Vol. 16, 2971–2974, 2017, doi: 10.1109/LAWP.2017.2756093.
14. Pozar, D. M., *Microwave Engineering*, 3rd Edition, Wiley, New York, NY, USA, 2004.
15. Xu, F. and K. Wu, "Guided-wave and leakage characteristics of substrate integrated waveguide," *IEEE Trans. Microw. Theory Tech.*, Vol. 53, No. 1, 66–73, 2005.
16. Lai, Q., C. Fumeaus, W. Hong, and R. Vahldieck, "Characterization of the propagation properties of the half-mode substrate integrated waveguide," *IEEE Transactions on Antennas and Propagation*, Vol. 57, No. 8, 1996–2004, 2009.